

Object-based Bilateral Telemanipulation Between Dissimilar Kinematic Structures

G. Salvietti¹, L. Meli^{1,2}, G. Gioioso^{1,2}, M. Malvezzi² and D. Prattichizzo^{1,2}

Abstract—This paper presents a bilateral telemanipulation framework where the master and slave sub-systems have different kinematic structures. A virtual object is defined on the master and slave sides and used to capture the human hand motion and to compute the related force feedback. The force feedback is determined imposing that the same wrench acts on the master and slave virtual objects. An abstraction from the sub-system structures is obtained focusing on the effects produced on the manipulated object. The proposed approach has been tested with an experimental setup consisting of two haptic interfaces able to capture index and thumb motions on the master side and a DLR-HIT Hand II as slave sub-system.

I. INTRODUCTION

A bilateral telemanipulation system enables interaction between a human operator and an environment without requiring direct physical contact between them [1]. Ideally, the telemanipulation system is transparent to the user, i.e. does not distort the perception of the environment. The aim of transparency has to be pursued maintaining the closed-loop system stability regardless of the operator behaviour. These concepts are generally in contrast and a unique approach cannot be applied. Many solutions have been proposed to solve bilateral telemanipulation in a wide range of scenarios [2]. Tasks are usually performed by a mechanical manipulator (slave) remotely controlled by a human operator provided with a force reflecting interfaces (master). Haptic interfaces can, thus, enable the interaction with the remote environment. Kinematic structures of master and slave devices are typically different [3], [4]. Moreover, the complexity of the whole system increases when complex grippers or robotic hands are considered as slave devices and a force feedback is required on the human hand fingers [5], [6]. An universal kinematic interface, independent from the device structures, is needed to solve kinematic asymmetries. However, while different solutions have been proposed to map human hand configurations onto robotic hand with dissimilar kinematics [7], [8], there are few studies on how to compute the correct force feedback.

In this work we present a telemanipulation framework that can deal with kinematic asymmetries between master and slave structures. A new approach for force feedback

The research leading to these results has received funding from the European Union Seventh Framework Programme FP7/2007-2013 under grant agreement n 270460 of the project “ACTIVE - Active Constraints Technologies for Ill-defined or Volatile Environments”.

¹Department of Advanced Robotics, Istituto Italiano di Tecnologia, via Morego, 30, 16163 Genova, Italy gionata.salvietti@iit.it

²Università degli Studi di Siena, Dipartimento di Ingegneria dell’Informazione e Scienze Matematiche, Via Roma 56, 53100 Siena, Italy. {meli, gioioso, malvezzi, prattichizzo}@dii.unisi.it

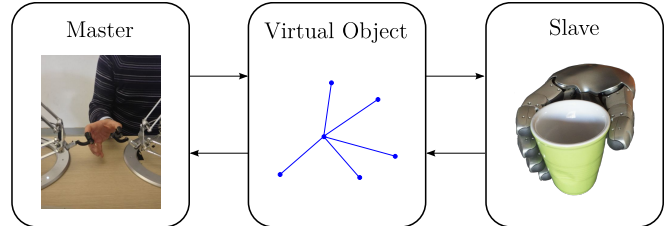


Fig. 1: Working principle of the proposed telemanipulation algorithm. The virtual object is used to map the human hand motion and to compute the force feedback.

computation is considered. The main idea is to define two virtual objects on both the master and the slave sides and to impose a correspondence between the twist/wrench applied on these objects. Such correspondence provides basic building blocks to translate human hand motions into movements of a robotic hand, as well as to compute the correct force to be rendered by the haptic devices. The proposed approach is both sufficiently abstract to overcome the discrepancies between human and robot kinematics and dynamics, and enough simple to be executed in real-time. For the sake of simplicity, we focused only on in-hand manipulation assuming the real object on the slave side already grasped. We tested our approach using two Omega.3 haptic devices by Force Dimension as master device and a robotic DLR-HIT Hand II [9] as slave device.

The paper is organized as it follows. Section II summarizes the main equations of robotic grasping used in the teleoperation framework. Section III deals with the description of how the motions of the master devices are mapped onto the slave one and how the force feedback is computed. In Section IV the setup used to validate the approach is outlined, while in Section V the experimental results are presented and discussed. Finally Section VI addresses concluding remarks and future works.

II. GRASPING BACKGROUND

In this section we summarize the main equations necessary to define grasp properties. Further details on robotic grasp theory can be found in [10].

Let us consider a generic hand grasping an object with nc contact points. Two reference frames, $\{N\}$ and $\{B\}$, are respectively defined on the hand palm and on the grasped object. The vector $u = [o^T \ \phi^T]^T \in \mathfrak{R}^6$ describes the information on the relative configuration between such frames. The vector $o \in \mathfrak{R}^3$ denotes $\{B\}$ origin position with respect to $\{N\}$, and

$\phi \in \mathfrak{R}^3$ is a vector describing their relative orientation. In a quasi-static framework, the external load wrench applied to the object, indicated with w , is balanced by the contact forces, whose components are collected in the contact force vector λ . The dimension of this vector depends on the model adopted to describe the contact. In this paper we consider a Hard Finger (HF) contact model [10]. With this type of model, at each contact point w has three force components and no moments, then the dimension of the contact force vector λ is $n_l = 3nc$. The force and moment equilibrium equation for the object is described by the following equation

$$w = -G\lambda, \quad (1)$$

where $G \in \mathfrak{R}^{6 \times n_l}$ is the grasp matrix. For a complete discussion of the contact models and the definition of the grasp matrix G , the reader is referred to [10]. By applying the static-kinematic duality relationship, we can express a generic displacement of the contact points on the object $\Delta p_o \in \mathfrak{R}^{n_l}$ as a function of the object displacement Δu as

$$\Delta p_o = G^T \Delta u. \quad (2)$$

Solving eq. (1) for the contact forces we obtain

$$\lambda = -G^\# w + N_G \zeta, \quad (3)$$

where $G^\#$ is the pseudoinverse of grasp matrix, $N_G \in \mathfrak{R}^{n_l \times h}$ is a matrix whose columns form a basis for the nullspace of G and $\zeta \in \mathfrak{R}^h$ is a vector parametrizing the homogeneous part of the solution. The generic solution of the homogeneous part $\lambda_{hom} = N_G \zeta$, represents a set of contact forces whose resultant force and moment are zero, and are referred to as internal forces. The structure of the hand has to be considered to define which internal forces can be actively controlled [11]. The relationship between hand joint torques $\tau \in \mathfrak{R}^{n_q}$, where n_q is the number of actuated joints, and contact forces is:

$$\tau = J^T \lambda, \quad (4)$$

where $J \in \mathfrak{R}^{n_l \times n_q}$ is the hand Jacobian matrix. The hand Jacobian relates the contact point displacements on the hand Δp_h to the joint variable variations Δq

$$\Delta p_h = J \Delta q.$$

Details on the definition and computation of hand Jacobian matrix, can be found in [10]. Introducing compliance in the model is necessary to solve the problem of force distribution when the grasp is statically indeterminate or hyperstatic [10] and to consider local deformation at contact as well as compliance at joint actuation level. Starting from an initial equilibrium condition, the contact force variation is expressed as

$$\Delta \lambda = K_c (J \Delta q - G^T \Delta u), \quad (5)$$

where $K_c \in \mathfrak{R}^{n_l \times n_l}$ represents the contact stiffness matrix. If we consider the joint compliance [12], the joint torques can be expressed as

$$\Delta \tau = K_q (\Delta q_{ref} - \Delta q),$$

where $K_q \in \mathfrak{R}^{n_q \times n_q}$ is the joint stiffness matrix and Δq_{ref} is the variation of the joint reference value. Let us assume to

have a grasp in an initial reference equilibrium configuration, and to apply a small change of the hand joint reference values Δq_{ref} . By linearising the general equilibrium relationships in eq. (1) and (4), it is possible to evaluate the corresponding configuration variation. In particular, the relative object displacement Δu is given by

$$\Delta u = V \Delta q_{ref}, \quad (6)$$

where $V = (GKG^T)^{-1}GKJ$, $V \in \mathfrak{R}^{6 \times n_q}$. The equivalent stiffness K can be evaluated as $K = (K_c^{-1} + JK_qJ^T)^{-1}$ [12]. Similarly, the contact force variation $\Delta \lambda$ generated by Δq_{ref} can be evaluated as

$$\Delta \lambda = P \Delta q_{ref}, \quad (7)$$

where $P = (I - G_K^\# G)KJ$, $P \in \mathfrak{R}^{n_l \times n_q}$, with $G_K^\#$ pseudoinverse of grasp matrix G weighted with the stiffness matrix K [11]. Eq. (7) defines the relationship between the input joint reference variations and the corresponding contact force variation. A basis matrix E for the subspace of controllable internal forces can be therefore defined as

$$\mathcal{R}(E) = \mathcal{R}((I - G_K^\# G)KJ),$$

with $\mathcal{R}()$ representing the image space. Eq. (6) shows how the object displacements Δu can be controlled from one equilibrium configuration to another by modifying joint reference values Δq_{ref} . Among all the possible motions of the grasped objects, rigid-body motions are relevant since they do not involve visco-elastic deformations in the contact points. Considering eq. (5) and imposing $\Delta \lambda = 0$, the rigid body motion can be obtained by solving the homogeneous system

$$[J \quad -G^T] \begin{bmatrix} \Delta q \\ \Delta u \end{bmatrix} = 0.$$

Let us then define a matrix Γ , whose columns form a basis of such subspace. Under the hypothesis that the object motion is not indeterminate [10], i.e. $\mathcal{N}(G^T) = \emptyset$, meaning that the object is completely restrained by contacts, neither redundant, i.e. $\mathcal{N}(J) = \emptyset$, matrix Γ can be expressed as

$$\Gamma = \mathcal{N} \begin{bmatrix} J & -G^T \end{bmatrix} = \begin{bmatrix} \Gamma_{qc} \\ \Gamma_{uc} \end{bmatrix}, \quad (8)$$

where the image spaces of Γ_{uc} and Γ_{qc} consist of coordinated rigid-body motions of the mechanism, for the hand joint references and the object position and orientation, respectively. It is worth to recall that $\mathcal{R}(\Gamma_{uc}) \subseteq \mathcal{R}(V)$, i.e. rigid-body motions of the object are not all the possible controllable object motions.

III. TELEMANIPULATION FRAMEWORK

This paper focuses on bilateral telemanipulation between dissimilar kinematics. Grasps with multiple contacts are taken into account. We assume the object in the slave side already stably grasped. Only two reference points are tracked, index and thumb fingertips, using two 3 DOF haptic interfaces. More than two contact points are allowed between the robotic hand and the real object. To overcome the problem due to different numbers of contact points on

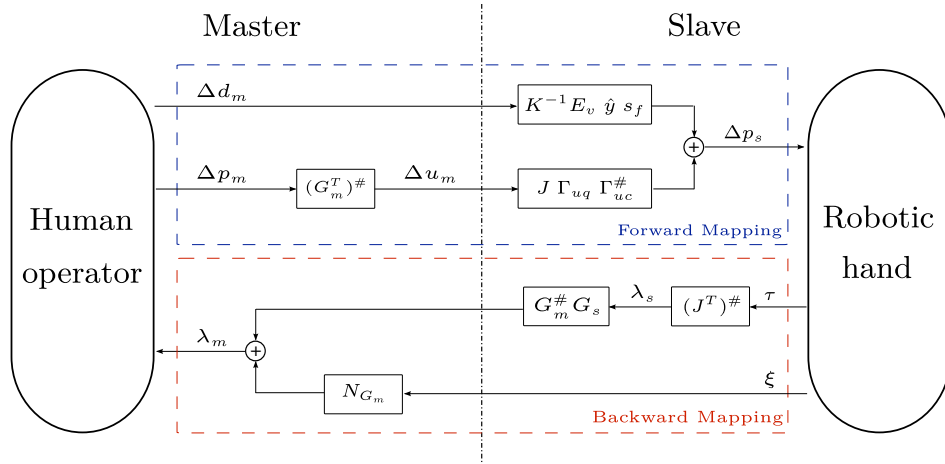


Fig. 2: Schematic overview of the proposed bilateral telemanipulation framework. The *forward mapping* defines how to move a remote robotic hand, given the norm of the distance between the haptic device end-effectors on the master side and the position of a virtual object grasped with them. The *backward mapping* renders the forces perceived by the slave sub-system on the haptic interfaces.

the master and on the slave sides, the presented method is designed in the object domain. We exploited the main entities relevant for the robotic grasping introduced in the previous section considering two separate problems: the control of the internal forces and the rigid body motion of the object. In this paper we do not discuss about the passivity layer which is designed using well known techniques, based on [13].

In the rest of the section we describe how the proposed telemanipulation framework can be used abstracting from master and slave kinematics. We refer to *forward mapping* to indicate all the passages necessary to reproduce the motion captured in the master side in the slave side. All the procedures needed to map forces measured on the slave side onto the master side are referred to as *backward mapping*. In Fig. 2 a scheme of the telemanipulation framework is reported.

A. Forward mapping

There are several solutions in literature that deal with mapping a master device motion onto a slave device. Using fingertip mapping [14] or pose mapping [15] it is possible to track only certain important points on the hand and to try to reproduce their motion on the robotic hand. These solutions can be implemented when the number of tracked reference points is equal or bigger on the master side than on the slave side. Consider for instance a tracking system able to track only two fingertips on the master side and an anthropomorphic robotic hand on the slave side with 5 fingers. The problem can be solved only introducing some heuristic to estimate the robot hand motion [16]. When the force feedback is considered it is difficult to use the same heuristics since they could lead to unexpected behaviours on the master side. For these reasons, we consider the effects on a virtual object instead of the single contribution of the fingers. This solution allows to generalize the algorithm to different contact points number and positions without focusing on the kinematic of master and slave sides.

Let $\{N_m\}$ indicate the reference frame set on the base of one device and let $p_{1,m}$ and $p_{2,m}$ represent the position of the two device end-effectors, both computed with respect to $\{N_m\}$ as showed in Fig. 3a. The virtual object is obtained considering the line connecting the two fingertips as pictorially represented in Fig. 3b. Let us indicate with d_m the norm of the distance between the two fingertips, i.e. $d_m = \|p_{2,m} - p_{1,m}\|$. Note that the virtual object idea can be extended to an arbitrary number of reference points by considering for instance a sphere as virtual object defined as the minimum volume sphere containing the reference points [7].

Let $\{B_m\}$ represent a reference frame of the virtual object (see Fig. 3b). $o_m \in \mathfrak{R}^3$ denotes the position of $\{B_m\}$ origin with respect to $\{N_m\}$. The object center o_m is considered as the mid-point between the two haptic device end-effectors. Consider also $\phi_m \in \mathfrak{R}^3$ a vector describing the relative orientation between the frames (e.g. Euler angles). Let furthermore $u_m = [o_m^T \ \phi_m^T]^T \in \mathfrak{R}^6$ collects information on position and orientation between the above mentioned frames.

Starting from an equilibrium configuration and considering a small change of the hand posture it is possible to evaluate from eq. (2) the corresponding object displacement Δu_m as

$$\Delta u_m = (G_m^T)^\# \Delta p_m + N_{G_m^T} \psi,$$

where $p_m = [p_{1,m}^T \ p_{2,m}^T]^T \in \mathfrak{R}^6$ groups the two reference points on the master side, $N_{G_m^T}$ is a matrix whose columns form a basis of $\mathcal{N}(G_m^T)$ and the vector ψ parametrizes the homogeneous solution to the equilibrium problem described in eq. (2). Considering the particular configuration of the master sub-system proposed in this work and the contact model used (HF), the nullspace of G_m^T matrix is not empty. However, we did not consider this aspect since the available Omega.3 cannot provide measures about the rotation along the axis connecting the two reference points.

Consider now the robotic hand on the slave side grasping

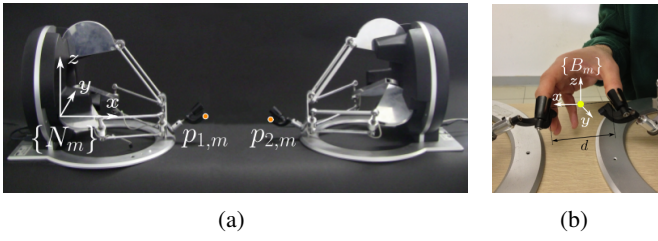


Fig. 3: The master sub-system setup. (a) Two Omega.3 haptic devices. Both $p_{1,m}$ and $p_{2,m}$ are expressed with respect to the same reference frame $\{N_m\}$. (b) The virtual object with its own reference frame $\{B_m\}$.

an object using nc_s contact points, and indicate with $p_s \in \mathcal{R}^{3nc_s}$ the resulting contact point location vector, expressed with respect to the reference frame $\{N_s\}$ depicted in Fig. 4a. A second virtual object is considered for the robotic hand. It is defined by the fingertip positions involved in the grasp of the real object. The virtual object center o_s is considered as the mean position between the contact points,

$$o_s = \frac{1}{nc_s} \sum_{i=1}^{nc_s} p_{i,s} .$$

Note that in this work the approaching phase is not considered since we are focusing on manipulation more than on grasping issues. We assumed to determine the same grasping matrix for the real and the virtual objects in the slave sub-system.

The final target of the forward mapping is to move the manipulated object accordingly to the virtual object defined on the master side, while guaranteeing the stability of the grasp in the slave sub-system. We considered a generic motion on the master side as a composition of a rigid body motion and a deformation of the virtual object, that can be related to an internal force contribution. The master rigid body motion is mapped on the slave one, while the internal force variation applied by the master sub-system is projected on the slave subspace of controllable internal forces. Therefore the motion decoupling allows to independently control both the component variations.

Referring to eq. (8), the rigid body contribution to the motion of the reference points on the slave side, can be computed as

$$\Delta p_{s, RB} = J \Gamma_{qc} \Gamma_{uc}^\# \Delta u_m , \quad (9)$$

where J is the Jacobian matrix of the slave device. To deal with different initial positions of haptic device end-effectors we introduced a scaling factor as

$$s_f = \frac{1}{nc_s d_m} \sum_{i=1}^{nc_s} \|p_{i,s} - o_s\| , \quad (10)$$

computed at the beginning of the telemanipulation task. Concerning the internal forces, the contribution in terms of reference point displacement can be obtained as

$$\Delta p_{s, IF} = K^{-1} E_v \hat{y} \Delta d_m s_f , \quad (11)$$

where $K \in \mathcal{R}^{3nc_s \times 3nc_s}$ is the contact points stiffness matrix, E_v is a matrix whose columns form a basis for the subspace



Fig. 4: The slave sub-system setup. (a) A DLR-HIT Hand II with the contact points $p_{i,s}$ ($i = 1, \dots, nc_s$) expressed with respect to the reference frame $\{N_s\}$. (b) The real cube with its own reference frame $\{B_s\}$.

$\mathcal{R}(PN_V)$, N_V is a matrix whose columns form a basis for the subspace $\mathcal{N}(V)$, \hat{y} is evaluated as $\hat{y} = (E_v)^\# n$, and $n \in \mathcal{R}^{3nc_s}$ is the vector of the normals to the contact surface. This part of the solution depends on the system compliance, defined through the stiffness matrix K , that takes into account both the contact and the joint compliance, as discussed in Sec. II. The projection on the $\mathcal{R}(PN_V)$ subspace avoids to move the object while the internal forces are modified, as detailed in [17]. The displacements defined in eq. (9) and (11) are related to the reference contact points. It is worth to observe that if the grasp of a real object is considered, the reference points ideally can move inside the object, while the real contact points lie on the surface. The penetration of the reference points inside the object is proportional to the contact force, according to the compliant model described in the previous section.

Combining eq. (9) and (11), we get the displacement of the reference points on the slave side

$$\Delta p_s = J \Gamma_q \Gamma_{uc}^\# \Delta u_m + K^{-1} E_v \hat{y} \Delta d_m s_f .$$

Finally, the displacement of the robotic hand joints Δq_s is computed as

$$\Delta q_s = J^\# \Delta p_s .$$

In this work we assumed that the robotic hand is not redundant, i.e. $\mathcal{N}(J) = \emptyset$.

B. Backward mapping

In this section, we describe how to evaluate the forces to be rendered on the master side. The final aim is to display the wrench acting on the real object grasped by the slave device to the user. This part of the solution does not consider the specific kinematics of the master and slave, but it focuses only on the effects imposed by the manipulated object.

Consider $\tau \in \mathcal{R}^{n_q}$ as the vector of the torques measured at the joints. It is possible to compute the forces at the contact points as

$$\lambda_s = (J^T)^\# \tau + N_{JT} \chi , \quad (12)$$

where N_{JT} is a matrix whose columns form a basis of $\mathcal{N}(J^T)$, and the vector χ parametrizes the homogeneous solution to the equilibrium problem described in eq. (4).

The corresponding wrench acting on the slave side can be estimated as

$$w_s = G_s \lambda_s ,$$

where G_s is the grasp matrix evaluated for the slave hand grasp. By imposing that the wrench to be rendered on the master virtual object w_m is the same applied at the slave side w_s and recalling eq. (3), the arising forces to be rendered by the haptic interfaces $\lambda_m \in \mathfrak{R}^{3n_{c_m}}$ are

$$\lambda_m = G_m^\# G_s \lambda_s + N_{G_m} \xi ,$$

where N_{G_m} is a matrix whose columns form a basis of $\mathcal{N}(G_m)$ and ξ is a vector parametrizing the homogeneous part of the solution. ξ can be selected considering the human hand skills in terms of joint torques and muscle activity as proposed in [18]. In this work $N_{G_m} \in \mathfrak{R}^{6 \times 1}$ and $\xi \in \mathfrak{R}$ since only two contact points are taken into account. We then evaluated ξ as

$$\|N_{G_m} \xi\| = \|(I - G_s^\# G_s) \lambda_s\| .$$

The term $\|(I - G_s^\# G_s) \lambda_s\|$ represents an estimation of the total amount of forces exerted on the real grasped object.

IV. EXPERIMENTAL SETUP

The proposed algorithm has been evaluated with a series of experiments carried out with a teleoperation system composed of two Omega.3 haptic devices on the master side and a DLR-HIT Hand II on the slave side. Each of the haptic interfaces has a thimble instead of the default end-effector to easily fit a human fingertip (see Fig. 3a). Since only in-hand manipulation was considered, the operator was asked to keep its wrist firm during the tasks execution. The position of the right interface is strictly related with the one on the left, since only a reference frame for the master side was used as introduced in Sec. III. A preliminary calibration test is therefore fundamental to place the devices in the correct positions, making coherent the whole master side in terms of reference frames. The object grasped by the DLR-HIT Hand II is a cube with a side of 3 cm, whose position was computed with respect to $\{B_s\}$ as shown in Fig. 4b.

A multi-thread software is built to let the heterogeneous interfaces communicate together since each controller presents a specific sampling rate. Since the robotic hand motors cannot follow such high sampling rate and the amount of data to be processed at each loop is too large for that speed, we set the refresh frequency of the slave sub-system f_s thread around 200 Hz. The difference in terms of sampling rate between the threads is exploited to manage possible force spikes on the master side. The force signals read from the robotic hand were smoothly applied to the human fingertips during the $\lfloor \frac{f_m}{f_s} \rfloor$ extra cycles on the master sub-system, with f_m as master frequency. In the same way, the position of the virtual object received by the robotic hand was evaluated as the mean between the positions tracked.

V. RESULTS

In order to validate the performances of the proposed framework, five male subjects, age range 24 – 30, all right-handed, took part to two experiments. Two of them had previous experience with haptic interfaces. None of the participants reported any deficiencies in their perception abilities. The participants were asked to wear the thimbles,

one on the thumb and one on the index finger and complete a proposed task.

The first experiment consisted in moving the virtual object on the master side and in replicating its displacement on the real cube, holding it with a three fingers grasp (i.e. the fingertips of thumb, index and middle finger). To emphasize the effectiveness of the rigid body motion contribution on the forward mapping procedure, the rendering of the internal forces was disabled. In this way, independently from how much the subject squeezed the virtual object on the master side, the initial internal force value of the slave side remained constant. Six virtual walls were introduced in order to avoid users to reach the boundaries of the robotic hand work-space, where joint singularities were experienced. This approach limits the work-space of the master devices, however since an in-hand manipulation was considered, these limitations did not significantly affect the experiments. Fig. 5a shows the trajectories of the virtual object and the real cube, considering for both $[0 \ 0 \ 0]^T$ as the initial position. Fig. 5b illustrates the sum of the absolute values of forces measured by all the robotic hand fingers and the sum of the absolute values of forces rendered by the haptic devices. Both the plot of x and z axis (see Fig. 3 and 4 for reference frame orientations) was nearly 0, as expected considering rigid body motion. The higher values on the y axis are due to the poor quality estimation of the contact forces using eq. (12).

In the second experiment, the backward mapping was validated. The subjects were asked to reduce the distance between the thimbles to squeeze the object grasped by the robotic hand. Fig. 6 reports the sum of the absolute value of forces applied on the user fingertips with respect to d_m . For the sake of clarity, we reported only two subjects in the plot. It is worth to underline that forces on the slave side are evaluated using three fingers, processed by the proposed algorithm and rendered on the two contact points on master side. The different slopes of the interpolation lines are related to the scaling factor considered (eq. (10)), since the two users started from two different initial positions. The bigger is the scaling factor, the higher is the force provided to the users with respect to specific value of d_m .

VI. CONCLUSION AND FUTURE WORK

In this paper a new telemanipulation framework that can deal with kinematic asymmetries between master and slave structures has been presented. The force feedback has been computed by imposing the same wrench estimated on the real grasped object on a virtual object defined on the master side. This solution focuses on the effects on the manipulated object and allows to abstract from the device kinematics. Two manipulation experiments have been proposed to validate the approach. We considered the object on the slave side already grasped by the robotic hand. This assumption was useful to define the grasp matrix for the real grasped object. A grasp approaching phase may be considered as an extension of the algorithm proposed. In the proposed approach, the human operator cannot directly control all the slave device motions. Regardless the number of contacts it has, slave device applies internal forces along directions belonging to the $\mathcal{N}(V)$ only, then allowing no object movements. Those directions are not

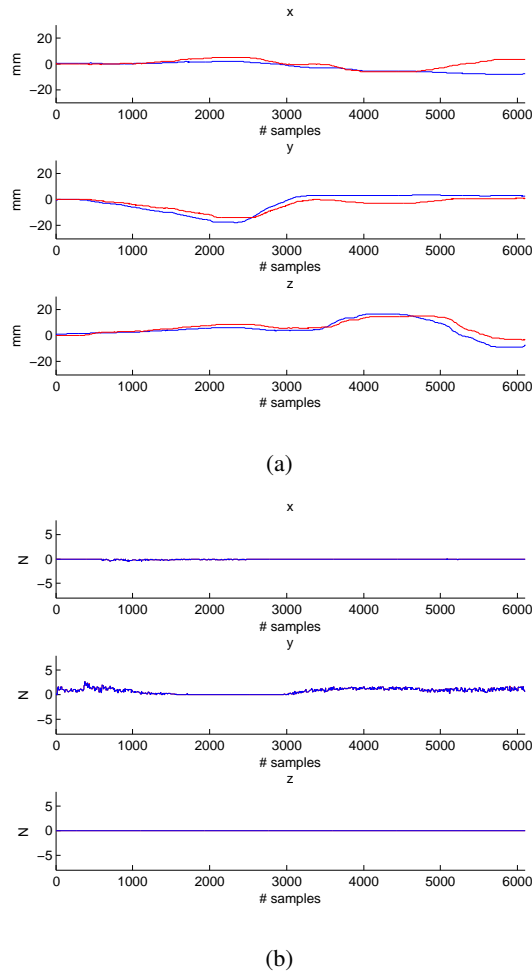


Fig. 5: Experiments for the forward mapping validation. (a) Trajectories of the virtual object on the master side (blue) and the cube in slave sub-system (red). (b) Sum of the absolute value of the forces evaluated by the robotic hand torque sensors (red), and the sum of the absolute value of the forces applied back on the Omega haptic devices (blue).

fixed or a priori chosen, but they are dynamically determined during the telemanipulation task. Similarly a movement on master side, is mapped onto $\mathcal{R}(\Gamma_{uc})$, thus only the rigid components are actively reproduced on the slave side. As future work we are testing different slave systems which can be useful for medical applications, especially when different sensor inputs have to be combined.

REFERENCES

- [1] J. E. Speich, K. Fite, and M. Goldfarb, "Transparency and stability robustness in two-channel bilateral telemanipulation," *Transactions of the ASME*, vol. 123, pp. 400–407, 2001.
- [2] P. F. Hokayem and M. W. Spong, "Bilateral teleoperation: An historical survey," *Automatica*, vol. 42, no. 12, pp. 2035–2057, 2006.
- [3] A. Peer, B. Stanczyk, and M. Buss, "Haptic telemanipulation with dissimilar kinematics," in *Proc. IEEE/RSJ Int. Conf. on Intelligent Robots and Systems*, 2005, pp. 3493–3498.
- [4] C. Pacchierotti, F. Chinello, M. Malvezzi, L. Meli, and D. Prattichizzo, "Two finger grasping simulation with cutaneous and kinesthetic force feedback," *Haptics: Perception, Devices, Mobility, and Communication. Eurohaptics*, pp. 373–382, 2012.

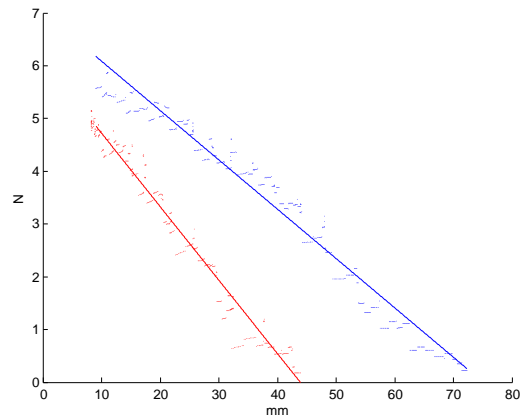


Fig. 6: Sum of the absolute value of the forces belonging to $\mathcal{N}(G_m)$ perceived by two users with respect to the norm of the distance between the haptic device end-effectors d_m . Different colors belong to different subjects. Raw data represented by dots are fitted with a linear interpolation to emphasize the proportion of the variables analysed.

- [5] W. B. Griffin, W. R. Provancher, and M. R. Cutkosky, "Feedback strategies for telemanipulation with shared control of object handling forces," *Presence: Teleoperators & Virtual Environments*, vol. 14, no. 6, pp. 720–731, 2005.
- [6] F. Kobayashi, G. Ikai, W. Fukui, and F. Kojima, "Two-fingered haptic device for robot hand teleoperation," *Journal of Robotics*, 2011.
- [7] G. Gioioso, G. Salvietti, M. Malvezzi, and D. Prattichizzo, "Mapping synergies from human to robotic hands with dissimilar kinematics: an approach in the object domain," *IEEE Trans. on Robotics*, 2013.
- [8] Y. Yoshimura and R. Ozawa, "A supervisory control system for a multi-fingered robotic hand using datagloves and a haptic device," in *Proc. IEEE/RSJ Int. Conf. on Intelligent Robots and Systems*, 2012, pp. 5414–5419.
- [9] H. Liu, K. Wu, P. Meusel, N. Seitz, G. Hirzinger, M. Jin, Y. Liu, S. Fan, T. Lan, and Z. Chen, "Multisensory five-finger dexterous hand: the DLR/HIT Hand II," in *Proc. IEEE/RSJ Int. Conf. on Intelligent Robots and Systems*, 2008, pp. 3692–3697.
- [10] D. Prattichizzo and J. Trinkle, "Grasping," in *Handbook on Robotics*, B. Siciliano and O. Kathib, Eds., 2008, pp. 671–700.
- [11] A. Bicchi, "Force distribution in multiple whole-limb manipulation," in *Proc. IEEE Int. Conf. on Robotics and Automation*, 1993, pp. 196–201.
- [12] M. R. Cutkosky and I. Kao, "Computing and controlling compliance of a robotic hand," *IEEE Trans. on Robotics and Automation*, vol. 5, no. 2, pp. 151–165, 1989.
- [13] M. Franken, S. Stramigioli, S. Misra, C. Secchi, and A. Macchelli, "Bilateral telemanipulation with time delays: A two-layer approach combining passivity and transparency," *IEEE Trans. on Robotics*, vol. 27, no. 4, pp. 741–756, 2011.
- [14] A. Peer, S. Eidenkel, and M. Buss, "Multi-fingered telemanipulation - mapping of a human hand to a three finger gripper," in *Proc. IEEE Int. Symp. in Robot and Human Interactive Communication*, 2008, pp. 465–470.
- [15] N. Y. Lii, Z. Chen, M. A. Roa, A. Maier, B. Pleintinger, and C. Borst, "Toward a task space framework for gesture commanded telemanipulation," in *Proc. IEEE Int. Symp. in Robot and Human Interactive Communication*, 2012, pp. 925–932.
- [16] J. Liu and Y. Zhang, "Mapping human hand motion to dexterous robotic hand," in *Proc. IEEE Int. Conf. on Robotics and Biomimetics*, 2007, pp. 829–834.
- [17] D. Prattichizzo, M. Malvezzi, M. Aggravi, and T. Wimbock, "Object motion-decoupled internal force control for a compliant multifingered hand," in *Proc. IEEE Int. Conf. on Robotics and Automation*, 2012, pp. 1508–1513.
- [18] G. Baud-Bovy, D. Prattichizzo, and N. Brogi, "Does torque minimization yield a stable human grasp?" *Multi-point Interaction with Real and Virtual Objects*, pp. 21–40, 2005.